17th World Conference on Earthquake Engineering, 17WCEE

Sendai, Japan - September 13th to 18th 2020

PREDICTION METHOD OF ENERGY DISTRIBUTION OF NONLINEAR VISCOUS DAMPERS FOR HIGH-RISE BUILDING

X. Liu [(1)], D. Sato[(2)], R. Okada[(3)]

[(1)] *Graduate Student, Tokyo Institute of Technology, Japan, liu.x.ar@m.titech.ac.jp*
[(2)] *Assco.Professor, FIRST,Tokyo Institute of Technology, Japan, sato.d.aa@m.titech.ac.jp*
[(3)] *Former graduate Student, Tokyo Institute of Technology, Japan, okada.r.af@m.titech.ac.jp*

Abstract

The use of passive control structure is increasing in recent years. The time history analysis method and the earthquake-resistant design method based on energy balance (energy method) are adopted for the design of passive control structure. However, the viscous damper which is the most frequently used as a passive control member is not included in Japan's current energy method notice. If the seismic response of the structure with viscous damper can be evaluated by energy method, it will help to expand the application range of the notice.

There are many researches on energy method. Akiyama proposed the prediction method of damage distribution of each story. Harada et al. proposed a prediction method of energy distribution of liner viscous dampers (linear prediction method) based on energy method. Arii et al. applied the prediction method to nonlinear viscous dampers by using Maxwell model and verified the accuracy of the prediction method. However, only the dampers with the velocity exponent (α) of 0.6 had been considered in the research of Arii, the dampers with small velocity exponent, had not been discussed. Because the use of the nonlinear viscous dampers is more than linear viscous dampers, it is necessary to research the prediction method of nonlinear viscous dampers.

In this paper, nonlinear viscous dampers were simulated by Maxwell model. The distribution cases of viscous dampers were defined by shear coefficient of dampers (α_{v1}). The accuracy of linear prediction method of viscous dampers was verified by comparing the value with the result by time history. From Fig.1 (a), it can be seen that when the velocity exponent is small, the accuracy of linear prediction is low. In addition, a nonlinear prediction method based on energy balance was proposed for linear viscous dampers as well as nonlinear viscous dampers. The viscosity coefficient of nonlinear viscous damper is equivalently linearized through energy equivalent. From Fig.1 (b), it can be seen that the accuracy of the nonlinear prediction method for the linear and nonlinear viscous dampers is better than the linear prediction method.

(i) α_{v1}= 0.01　(ii) α_{v1}= 0.05　(iii) α_{v1}= 0.10
(a) α=1.00

(i) α_{v1}= 0.01　(ii) α_{v1}= 0.05　(iii) α_{v1}= 0.10
(b) α=0.20

Fig.1 Distribution coefficient of viscous dampers (CH1)

Keywords: prediction method, energy distribution coefficient, nonlinear viscous damper, energy method

1. Introduction

The use of passive control structure is increasing in recent years. The time history analysis method and the earthquake-resistant design method based on energy balance (energy method) [1] are adopted for the design of vibration control buildings. However, the viscous dampers which is the most frequently used as a passive control member are not included in Japan's current energy method notice [2]. If the seismic response of the structure with viscous damper can be evaluated by energy method, it will helpful for expanding the application range of the notice.

There are many researches on energy method are carried out. Akiyama [1] proposed the prediction method of damage distribution of each story. Harada et al. proposed a prediction method of energy distribution of liner viscous dampers (linear prediction method) based on energy method [3]. Arii et al. applied the prediction method to nonlinear viscous dampers by using Maxwell model to simulate the viscous damper and verified the accuracy of the prediction method [4]. However, only the dampers with the velocity exponent (α) of 0.6 had been considered in the research of Arii, the dampers with small velocity exponent, have not been discussed. Because the use of the nonlinear viscous dampers is more than linear viscous dampers, it is necessary to research the prediction method of nonlinear viscous dampers.

This paper focuses on prediction method of energy distribution for nonlinear viscous dampers with different velocity exponents, around 1.0～0.2. The first part of the paper illustrates the analysis conditions of the structure, the earthquake, the parameters and distribution of the dampers. The second part presents the linear prediction method of the viscous damper and verified the accuracy of this method. The third part presents the nonlinear prediction method of the viscous dampers and the accuracy of the method is also verified. The last part is the conclusion.

2. Analysis condition

2.1 Structure

The height of the steel-frame building is 82.0m, 20-stories [5]. Fig.1 presents the plan and elevation of the building. The long side direction of the structure is the X direction, and the short side direction is the Y direction. The X direction is considered in this paper. Table 1 presents the members of the building. The 1st and 2nd periods T_f (X direction) are 2.29s and 0.81s. In order to consider the energy distribution of the dampers, the structural damping is set to 0 and the structure is elastic.

Table 1-Members of the building

Parts	Member
Columun	□-500×500×19×19 ~ □-800×800×36×36
Beam	H-750×250×14×25 ~ H-850×300×16×32

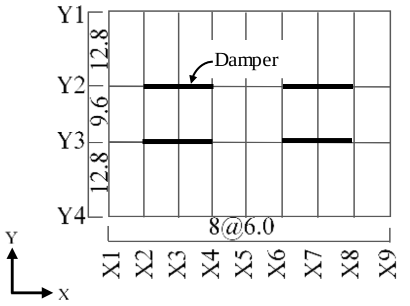

(a) Plan

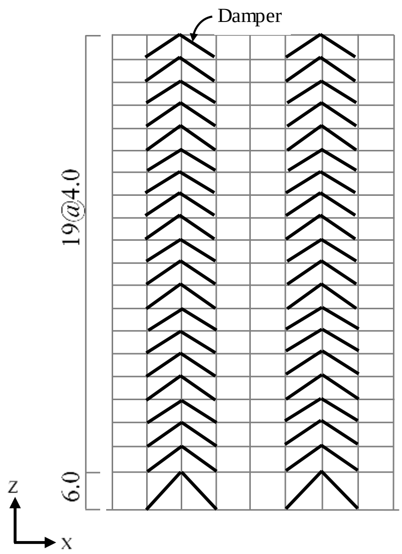

(b) Elevation

Fig. 1-Plan and Elevation (m)

2.2 Earthquake

Three earthquakes were selected in this paper. Art-Hachi (phase value: HACHINOHE 1968 EW), which is equivalent to an earthquake of level 2, and the long-period ground motion CH1[6] and SAN [6]. Fig.2 shows the acceleration of earthquakes. Fig.3 (a), (b) presents the pseudo-velocity response spectrum ${}_pS_v$ (h = 5 %) and energy spectrum V_E (h = 10 %).

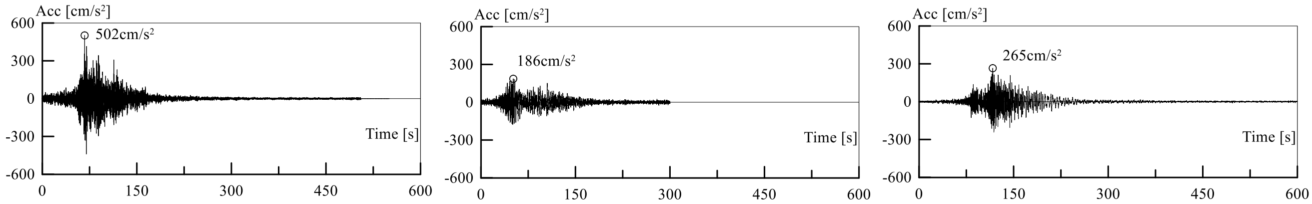

(a) Art-Hachi (b) SAN (c) CH1

Fig. 2-Acceleration of earthquakes

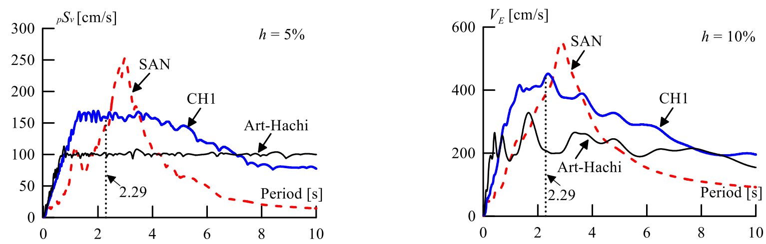

(a) Pseudo-velocity response spectrum (b) Energy spectrum

Fig. 3-Response spectrum

2.3 Viscous damper

Dampers and the support members are connected in series (Fig.4) [7], where $\hat{K}_d$ is the internal stiffness of damper in axis direction, $\hat{K}_b$ is the support member stiffness and $\hat{K}_b^*$ given by Eq.(1) is the equivalent stiffness of damper in axis direction. β is the internal stiffness coefficient and $\hat{C}_d$ is the viscosity coefficient in axis direction. In addition, it has been confirmed in previous studies[3] that the change in $\hat{K}_b^*$ has little effect on the energy distribution of the viscous damper, so this paper considered the equivalent support stiffness $\hat{K}_b^*$ to be rigid (β = 30000 [$m^{\alpha-1}/s^{\alpha}$] [7]).

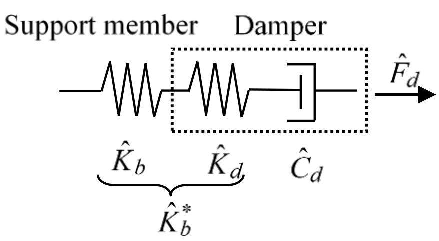

Fig. 4-Damper and support member

$$\hat{K}_{bi}^* = \beta \times \hat{C}_{di} \tag{1}$$

Shear coefficient of damper α_{v1} is expressed by Eq.(2). Where, W_f is the weight of the structure and F_{dD1} given by Eq.(3) is the horizontal force of all dashpot when the story drift angle of the first story R_{D1} is 1/100.

$$\alpha_{v1} = \frac{F_{dD1}}{W_f} \tag{2}$$

$$F_{dD1} = N_{d1} \cdot \hat{F}_{dD1} \cdot \cos\theta_{d1} \tag{3}$$

Where, N_{d1} is the number of the dampers in the first story, θ_{d1} is the angle of damper in the first story and $\hat{F}_{dD1}$ given by Eq.(4) [7] is the force of individual damper in the axis direction.

$$\hat{F}_{dD1} = \hat{u}_{dD1} \cdot \hat{K}''_{d1} \tag{4}$$

Where, $\hat{u}_{dD1}$ is the displacement of dashpot in axis direction when R_{D1} is 1/100, $\hat{K}''_{d1}$ is the loss stiffness of damper which can be expressed by Eq.(5) [7].

$$\hat{K}''_{d1} = \frac{\hat{C}_{d1} \cdot \omega^{\alpha}}{\hat{u}_{dD1}^{1-\alpha}} \tag{5}$$

Where, $\hat{C}_{d1}$ is the viscosity coefficient in axis direction of the dampers in the first story and ω is the first circular frequency of the structure. Since the support member is assumed to be rigid, the displacement is small, $\hat{u}_{dD1}$ can be given by Eq.(6).

$$\hat{u}_{dD1} \approx \hat{u}_{aD1} = \frac{\delta_{D1}}{\cos\theta_{d1}} = \frac{R_{D1} \cdot H_1}{\cos\theta_{d1}} \tag{6}$$

Where, δ_{D1} is the displacement and H_1 is the height of the first story. α_{d1} is obtained by Eq.(7) through submitting Eq.(3)~(6) into Eq.(2).

$$\alpha_{v1} = \frac{N_{d1} \cdot \hat{C}_{d1} \cdot \omega^{\alpha} \cdot (R_{D1} \cdot H_1)^{\alpha} \cdot \cos^{1-\alpha}\theta_{d1}}{W_f} \tag{7}$$

5 velocity exponents α (1.00, 0.80, 0.60, 0.38, 0.20) with 3 shear coefficients of damper in the first story α_{v1}(0.01, 0.05, 0.10) were considered. According to Eq.(7), $\hat{C}_{d1}$ can be obtained. $\hat{C}_d$ in the 5th ,9th ,13th,17th story were determined by multiplying the design story shear ratio Q_i/Q_1 with $\hat{C}_{d1}$. Q_i/Q_1 can be expressed by the distribution of seismic shear coefficient A_i (Eq.8) [8]. The uniform $\hat{C}_d$ are adopted in the 1st ~4th ,5th ~8th ,9th ~12th ,13th ~16th ,17th ~20th story. Fig.5 shows the distribution of $\hat{C}_{di}$ in the height direction. In Eq.(9), W_{fj} is the weight of j story.

$$A_i = 1 + \left(\frac{1}{\sqrt{\alpha_i}} - \alpha_i\right) \cdot \frac{2T_{f1}}{1 + 3T_{f1}} \tag{8}$$

$$\alpha_i = \frac{\sum_{i=j}^{20} W_{fj}}{W_f} \tag{9}$$

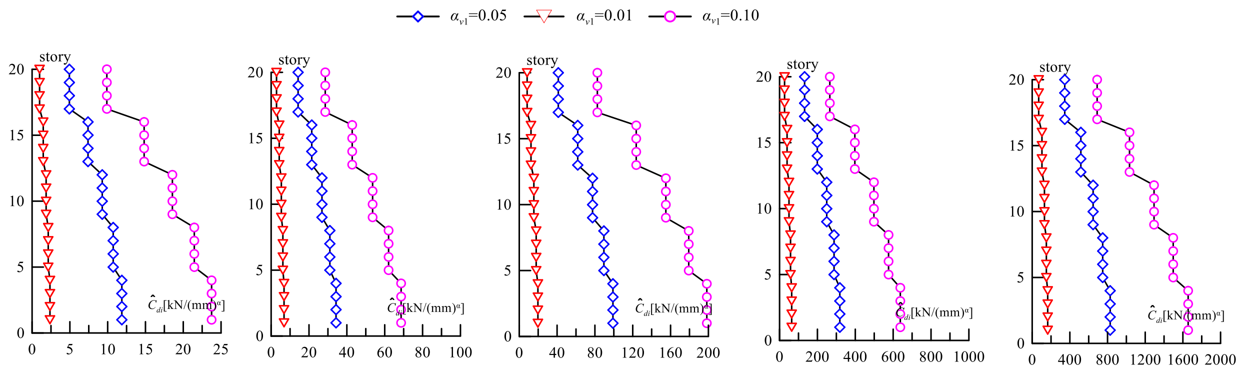

(a) α = 1.00 (b) α = 0.80 (c) α = 0.60 (d) α = 0.38 (e) α = 0.20

Fig. 5- Distribution of viscosity coefficient

3. Linear prediction method

3.1 Formulation for linear prediction method

The linear prediction method of the energy distribution of dampers is shown as Eq.(10) [3]. Where γ_d is the energy distribution coefficient of dampers, W_d is the energy absorbed by dampers. s_i' and h_i' is given by Eq.(11) [3]. Where M is the mass of the structure, m_i is the mass of i story, k_{fi} is the stiffness of i story, T_{f1} is the natural period of the structure and $\hat{C}_d$ is the viscosity coefficient in axis direction of the dampers. $\overline{\alpha_r}$ is the optimal distribution of yield-shear force coefficient and can be expressed by the strength distribution for the case of uniform cumulative inelastic deformation ratio[1]. In this paper, $\overline{\alpha_{ri}}$ is given by Eq.(12) [1].

In this section, the viscosity coefficient and energy absorbed by dampers are calculated dimensionless. Also, uniform numbers of equivalent repetition are adopted in each story. In addition, the maximum shear of the structure is approximately calculated according to the stiffness of the building and the maximum deformation of the dashpot.

$$\frac{1}{\gamma_{di}} = \frac{W_{di}}{\sum_{i=1}^{N} W_{di}} = \frac{s_i' \, h_i}{\sum_{i=1}^{N} s_i' \, h_i} \tag{10}$$

$$s_i' = \left(\sum_{j=i}^{N} \frac{m_j}{M} \right)^2 \times \overline{\alpha_{ri}}^2 \times \left(\frac{k_{f1}}{k_{fi}} \right)^2 \tag{11a}$$

$$h_i = \frac{\hat{C}_{di} T_{f1}}{4\pi M} \tag{11b}$$

$$\overline{\alpha_{ri}} = \begin{cases} 1+0.5x & 0 \le x \le 0.2 \\ 1+1.5927\,x - 11.8519\,x^2 + 42.5833\,x^3 - 59.4827\,x^4 + 30.1586\,x^5 & 0.2 < x < 1 \end{cases} \tag{12}$$

Where

$$x = \sum_{j=i}^{i-1} m_j / M \tag{13}$$

3.2 Verification

The accuracy of the prediction method is verified by comparing the predicted value with the time history analysis value (analytical value). In Fig.6, the energy distribution coefficient γ_{di} was shown. From Fig. 6(a)(i), it can be seen that when the α is 1.00 and α_{v1} is 0.01, the difference of analytical value under three earthquakes is small and the influence of earthquake on γ_{di} is less. The same tendency can be seen in other cases. However, when α is small and α_{v1} is large, bifurcate can be seen in the analytical value and the influence of time interval is considered (Appendix 1).

From Fig.6(a)(i) and Fig. 6(a)(iii), it can be seen that there is no effect on the prediction method due to α_{v1}. On the other hand, from Fig.6(c)(i) and Fig. 6(c)(iii), it can be seen that when α is 0.6, as α_{v1} increases, the accuracy of the method decrease. The same tendency can be seen from Fig.6(d) and Fig.6(e). Since W_d is excessively concentrated near the lower story, and the accuracy of this method tends to decrease accordingly. In addition, from Fig.6(a)(ii), Fig.6(b)(ii), Fig.6(c)(ii), Fig.6(d)(ii) and Fig.6(e)(ii), it can be seen that the smaller α is, the lower accuracy of the linear prediction method. As described above, the linear prediction method is only appropriate for linear viscous dampers. For the nonlinear viscous damper, the larger the α_{v1} and the smaller α is, the lower the accuracy of the linear prediction method.

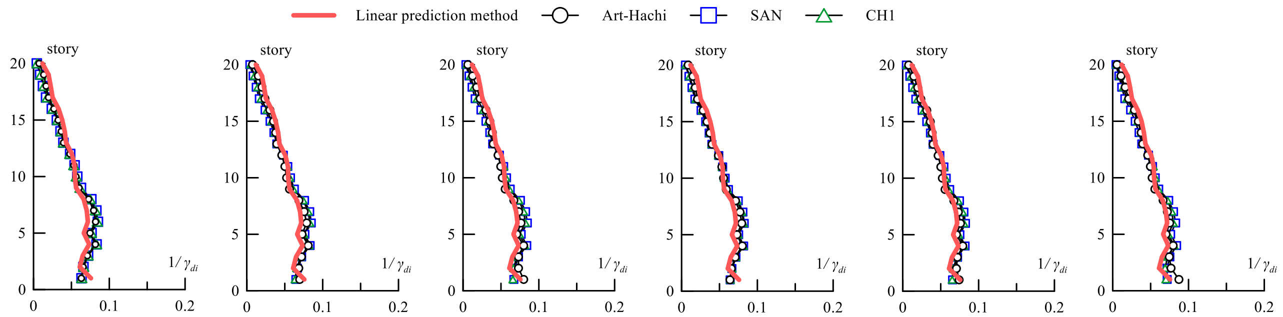

(i) α_{v1} = 0.01 (ii) α_{v1} = 0.05 (iii) α_{v1} = 0.10 (i) α_{v1} = 0.01 (ii) α_{v1} = 0.05 (iii) α_{v1} = 0.10

(a) α = 1.00 (b) α = 0.80

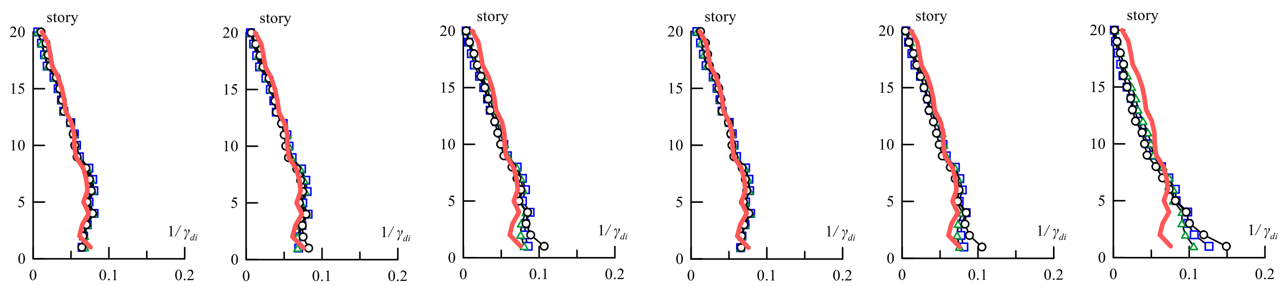

(i) α_{v1} = 0.01 (ii) α_{v1} = 0.05 (iii) α_{v1} = 0.10 (i) α_{v1} = 0.01 (ii) α_{v1} = 0.05 (iii) α_{v1} = 0.10

(c) α = 0.6 (d) α = 0.38

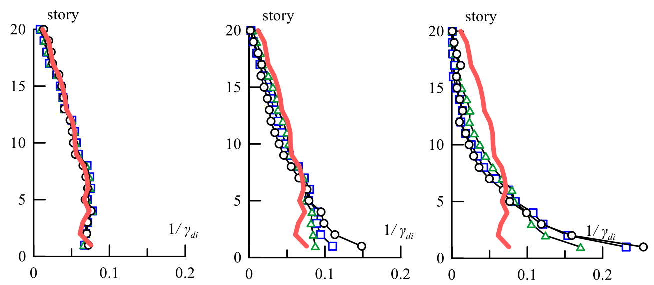

(i) α_{v1} = 0.01 (ii) α_{v1} = 0.05 (iii) α_{v1} = 0.10

(e) α = 0.2

Fig. 6- Accuracy of linear prediction method

4. Nonlinear prediction method

4.1 Formulation for nonlinear prediction method

As shown in Chapter 3, the linear prediction method is only appropriate for linear viscous dampers. In the case of highly nonlinear viscous dampers of which α is small, the accuracy of linear prediction significantly decreased. Therefore, in this part the nonlinear prediction method is proposed. The nonlinear prediction method is expressed by Eq.(14) [3] to Eq. (16). The one with "max" in the right subscript represents the maximum value. $\hat{u}_{di\max}$ is calculated by using the value from time history analysis. The optimal distribution of yield-shear force coefficient $\bar{\alpha}_{rd}$ and response shear coefficient of damper α_d in each story are shown as Eq.(17).

$$\frac{1}{\gamma_{di}} = \frac{W_{di}}{\sum_{i=1}^{N} W_{di}} = \frac{s_i'' h_{eqi}}{\sum_{i=1}^{N} s_i'' h_{eqi}} \tag{14}$$

$$s_i'' = \left(\sum_{j=i}^{N} \frac{m_j}{M} \right)^2 \times \bar{\alpha}_{rdi}^{\,2} \times \left(\frac{K_{d1}''}{K_{di}''} \right)^2 \tag{15a}$$

$$h_{eqi} = \frac{\hat{C}_{eqi} T_{f1}}{4\pi M} \tag{15b}$$

$$\hat{C}_{eqi} = \frac{4e^{-0.24\alpha} \hat{K}_{di}''}{\pi\ \omega} \tag{16a}$$

$$\hat{K}_{di}'' = \frac{\hat{C}_{di} \omega^{\alpha}}{\hat{u}_{di\max}^{1-\alpha}} \tag{16b}$$

$$\bar{\alpha}_{rdi} = \frac{\alpha_{di}}{\alpha_{d1}} \tag{17a}$$

$$\alpha_{di} = \frac{\hat{F}_{di\max}}{\sum_{j=i}^{N} m_j g} \tag{17b}$$

$$\hat{F}_{di\max} = \hat{K}_{di}'' \hat{u}_{di\max} \tag{17c}$$

As the nonlinear prediction method shown above, the equivalent viscosity coefficient $\hat{C}_{eq}$ is calculated by equivalently linearizing the viscosity coefficient of the nonlinear viscous damper. The followings showed how to calculate the equivalent viscosity coefficient. $\hat{C}_{eq}$ is determined by setting the absorbed energy W_d (Eq.18) of the nonlinear viscous damper the same with the absorbed energy W_{eq} (Eq.19) of the equivalent linearization viscous damper. It is assumed that the maximum deformation of the nonlinear viscous damper $\hat{u}_{di\max}$ is euqal to the maximum deformation of the equivalent linearization viscous damper $\hat{u}_{eqi\max}$ (Eq. 21).

$$W_{di} = 4e^{-0.24\alpha} n' \hat{K}_{di}'' \hat{u}_{di\max}^2 \tag{18}$$

$$W_{eqi} = \pi\ n' \hat{C}_{eqi} \omega\ \hat{u}_{eqi\max}^2 \tag{19}$$

$$W_{eqi} = W_{di} \tag{20}$$

$$\hat{u}_{eqi\max} = \hat{u}_{di\max} \tag{21}$$

4.2 Verification

In this part the accuracy of the linear prediction method and the nonlinear prediction method are verified. In Fig.7, a comparison of the energy distribution coefficient between the analytical value and the predicted value was shown. Since it was verified that the influence of earthquake on the energy distribution was small, the result under CH1 is shown as a representative.

From Fig.7(a)(i), it can be seen that the predicted value based on the nonlinear prediction method tended to more accurately than the linear prediction method. From Fig.7(a)(ii) and Fig.7(a)(iii), it can be seen that the accuracy of the nonlinear prediction method is slightly reduced, however the accuracy is better than the linear prediction method. In addition, there is no energy concentration occurs near the lower stories by the nonlinear method. From Fig.7(b)~(e), it can be seen that the larger α_{v1}, the lower accuracy of the nonlinear prediction method. However, the accuracy of nonlinear prediction method is better than linear prediction method. On the other hand, from Fig.7(a)(ii), Fig.7(b)(ii), Fig.7(c)(ii), Fig.7(d)(ii) and Fig.7(e)(ii), it can be seen that the smaller α, the lower accuracy of the nonlinear prediction method. The same tendency can be seen in other case. As described above, the accuracy of nonlinear prediction method is better than the linear prediction method. However, when α is small and α_{v1} is large, the accuracy of the nonlinear prediction method is not clear.

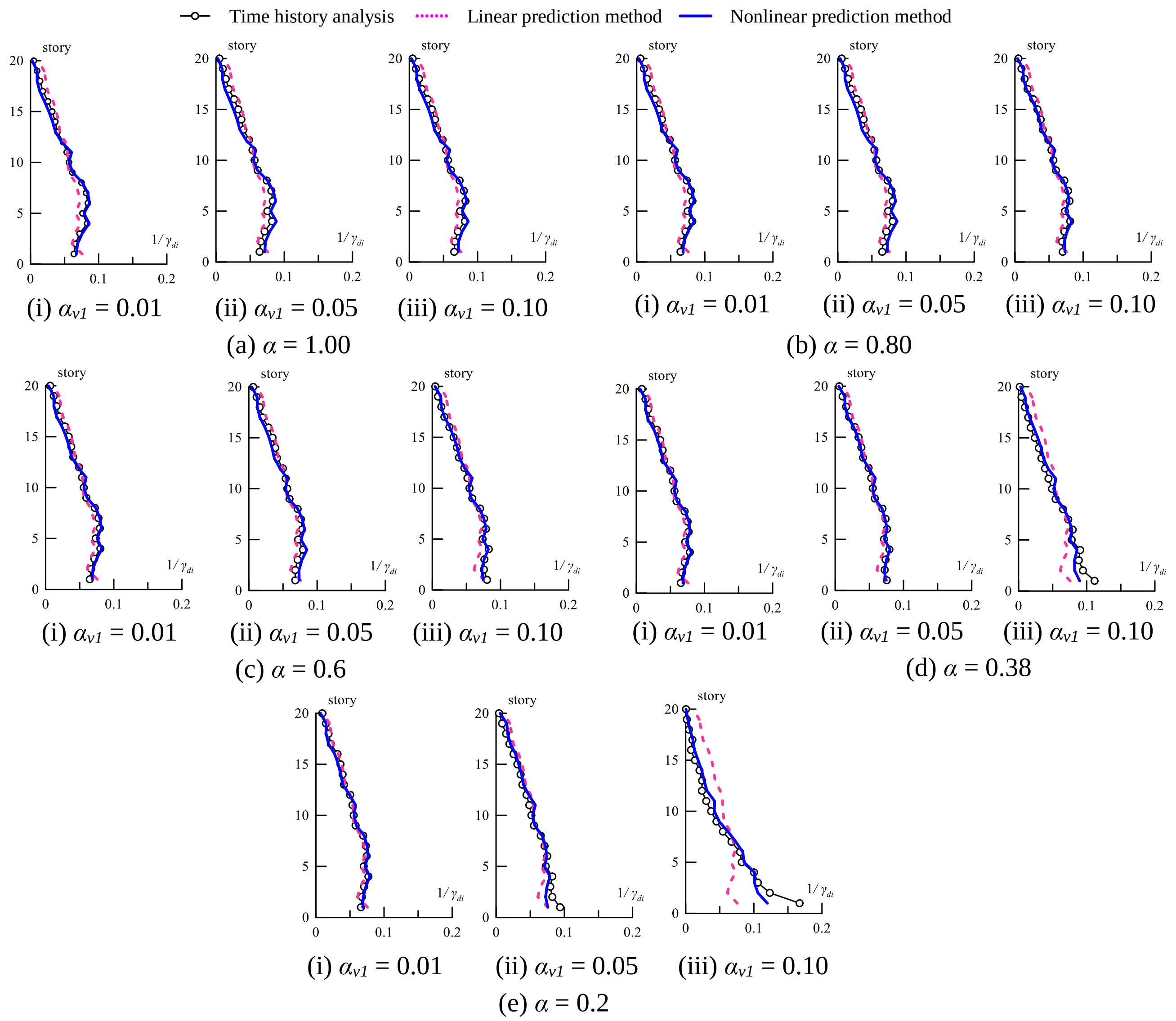

Fig. 7- Comparison of the energy dispersion coefficient (CH1)

5. Conclusions

In this paper, a nonlinear prediction method was proposed for viscous dampers. The viscosity coefficient of nonlinear viscous damper is equivalently linearized in this method. And the accuracy of linear prediction method and nonlinear prediction method of viscous dampers is also verified. The conclusions are as follows:
1) The influence of earthquake on the energy distribution of damper in the height direction is less.
2) The linear prediction method is only appropriate for linear viscous dampers. As for nonlinear viscous dampers, the accuracy is low.
3) The accuracy of the nonlinear prediction method for the linear and nonlinear viscous dampers is better than the linear prediction method. However, when the velocity exponent is small and shear coefficient of damper is large, the accuracy of the nonlinear prediction method not clear.

6. Acknowledgements

This work was supported by the JST Program on Open Innovation Platform with Enterprises, Research Institute and Academia.

7. References

[1] Akiyama, H., “Earthquake-Resistant Design Method for Buildings Based on Energy Balance,”Gihodo Shuppan Inc.,1999.[in Japanese]

[2] Wakita, N., Matsukage, T., Higuchi, K. and Nakamura, S., Structural Design By Energy Balance-Based Seismic Resistant Design : Introduction Of Design Realized Improvement Of Earthquake Performance And Economy. Nippon Steel Engineering technical review. Vol3.48-56.2012. [in Japanese]

[3] Haruda, Y., and Akiyama, H, Seismic Design of Flexible-stiff Mixed Frame with Energy Concentration, Journal of Structural and Construction Engineering, No.472, 57-66, 1995. [in Japanese]

[4] Arii, K., Sato, D., Matsukage, T. and Kitamura, H., Accuracy Evaluation of Energy Distribution Coefficient of Viscous Dampers, *AIJ Journal of Structural Engineering*, 88(I), 281-284, 2018.3. [in Japanese]

[5] Architectural Institute of Japan (AIJ), “Recommended Provision for Seismic Damping Systems applied to Steel Structures”, 2014. [in Japanese]

[6] Building Research Institute, http://www.kenken.go.jp/japanese/contents/topics/lpe/exponent.html (2017.6.30)

[7] The Japan Society of Seismic Isolation (JSSI),”Passive control structure design·construction manual”,2013. [in Japanese]

[8] Akenori, S., “Dynamic analysis of earthquake resistant structures,” Tohoku University Press,2010.

Appendix 1

The influence of time interval on the absorbed energy by dampers is shown in Fig.A1. From Fig.A1, it can be seen that the smaller the time interval, the better accuracy of the calculation.

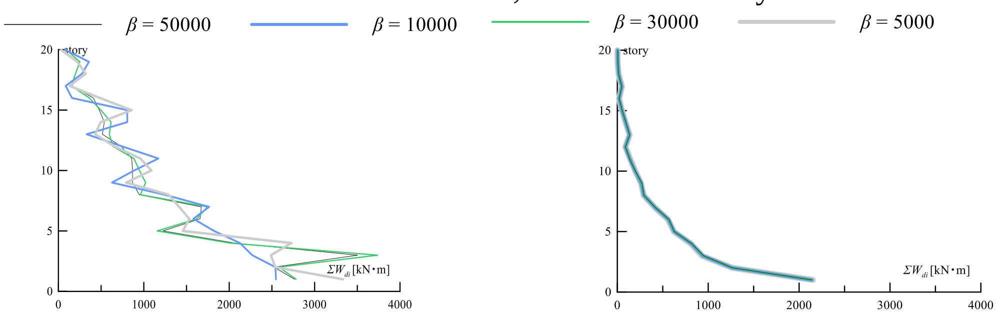

(a) Δt =0.0001 (b) Δt =0.00001

Fig.A1-Distribution of the absorbed energy by damper（α = 0.20, α_{d1} = 0.10）

